

Supporting Information

Controlling pyridinium-zwitterionic ligand ratio on atomically precise gold nanoclusters allowing for eradicating Gram-positive drug-resistant bacteria and retaining biocompatibility

Zeyang Pang^{1,2}, Qizhen Li¹, Yuexiao Jia¹, Weixiao Yan¹, Jie Qi¹, Yuan Guo³, Fupin Hu⁴, Dejian Zhou^{2}, and Xingyu Jiang^{1*}*

¹ Department of Biomedical Engineering, Southern University of Science and Technology, No 1088, Xueyuan Rd, Nanshan District, Shenzhen, Guangdong 518055, P. R. China.

² School of Chemistry and Astbury Centre for Structural Molecular Biology, University of Leeds, Leeds LS2 9JT, United Kingdom.

³ School of Food Science and Nutrition and Astbury Centre for Structural Molecular Biology, University of Leeds, Leeds LS2 9JT, United Kingdom.

⁴ Institute of Antibiotics, Huashan Hospital, Fudan University, Shanghai 200040, P. R. China.

I. EXPERIMENTAL SECTION

(A) Synthesis and characterisation of C5 ZW Ligand.

This synthetic method was mainly acquired from a previous report¹. According to this protocol, potassium thioacetate was reacted with 6-bromohexanoic acid to introduce a thiol acetate that was later hydrolysed to give a free thiol under essential condition.

Potassium thioacetate (3.5 g, 31.0 mmol, Alfa Aesar, <https://www.alfa.com/>) was mixed with 2.0 g (10.3 mmol) of 6-bromohexanoic acid (Alfa Aesar) in dimethylformamide (DMF, 100 mL) at ~ 0 °C under N₂ atmosphere. The mixture was left stirring overnight, with the temperature gradually warmed up to room temperature, producing a dark brown solution. The reaction mixture was rotary evaporated to remove most of the DMF, diluted with DCM (200 mL), and washed three times with acidic water (100 mL \times 3) (pH = 2). The organic layer was dried over Na₂SO₄ (Fisher Scientific, <https://www.fishersci.com/>), evaporated to dryness to give a dark brown crude product **C5-1** in >80% yield.

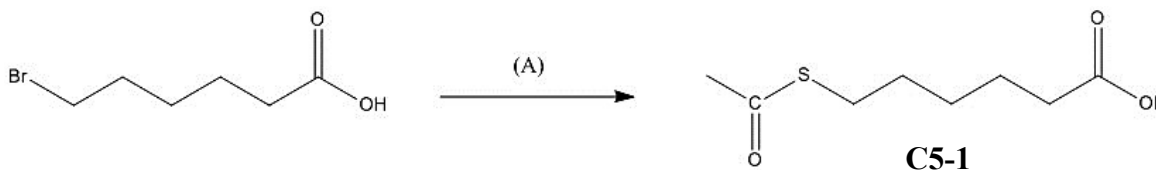


Figure S1. Scheme of replacement of the bromo group with thioacetate. (A) Potassium thioacetate, DMF, and 24 hours.

CDI (1,1'-Carbonyldiimidazole) was used in the second step as the amidation reagent to react with the carboxyl group to form intermediate (acyl imidazole), which subsequently reacted with an amine to form an amide bond².

C5-1 (0.50 g, 2.63 mmol) and CDI (0.64 g, 3.90 mmol, Alfa Aesar) were added in a two-necked round-bottomed flask with a magnetic stirring bar. The flask was purged with N₂ gas, and 10 mL of dry chloroform was added using a syringe. The mixture was left stirring for 1 h, transferred to an addition funnel, and added dropwise to a three-necked

flask containing 1.65 mL of N, N-dimethyl-1,3-propanediamine (Alfa Aesar) under N₂ at 0 °C. After stirring overnight, the reaction mixture was washed with saturated NaHCO₃ solution (10 mL × 3). The organic layer was dried over Na₂SO₄, and the solvent was evaporated to give a light orange waxy solid (**C5-2**) in ~ 100% yield, which was directly used in the next step.

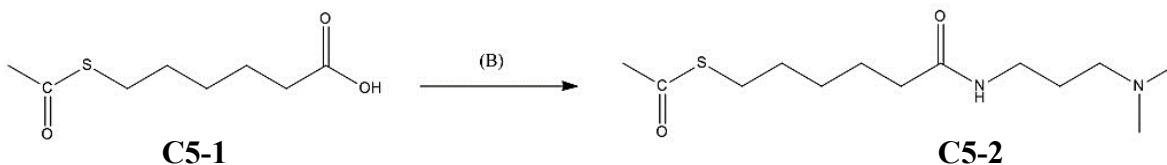


Figure S2. Amidation step of C5 preparation, producing C5-2. (B) CDI, N, N-dimethyl-1, 3-propanediamine, and dry chloroform.

C5-2 (0.6 g, 2.2 mmol) and 1,3-propanesultone (0.8 g, 6.6 mmol, Alfa Aesar) were added in a two-necked round-bottomed flask equipped with a magnetic stirring bar. 25 mL of dry chloroform was added to the flask, and the mixture was left stirring under N₂ at room temperature for two days. Then chloroform was evaporated to obtain a light orange residue named **C5-3**. The residue was washed several times with (tetrahydrofuran) THF to remove the excess of unreacted sultone. **C5-3** was dried under a vacuum. HPLC is performed with a gradient concentration (10%-90%) of methanol with water.

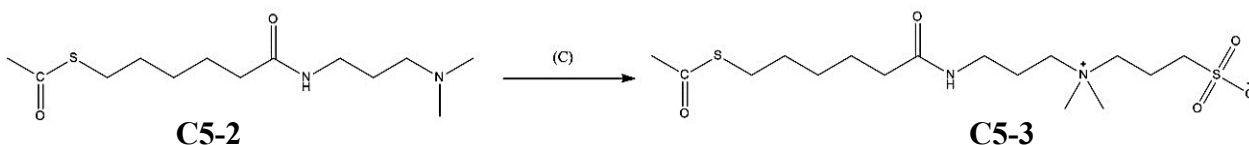


Figure S3. Synthetic route to C5 ZW ligand. (C) 1,3-propanesultone and dry CHCl₃

To get free thiol, 0.5 g of the ligand was dissolved in 5 mL of methanol. One equivalent of NaOH dissolved in 1 mL of water was injected into the solution, and the mixture was left stirring for 24 h under N₂. The product was neutralized by adding HCl (a few mL of 0.5 M solution). To collect the monothiol-zwitterion ligand, we dried the product under vacuum and re-dispersed it in methanol. The insoluble salts were precipitated out, and the clear supernatant liquid was collected. This process was repeated two times, yielding around 99%, **C5-4** is what we need. It is worth saying that the amidation step needs strict time control (overnight) because the alkaline of amine can

hydrolyse the thioacetate protection group to give free thiols. It was found that after stirring for two days at 35 °C, nearly all the thioacetate groups were deprotected and formed a disulfide bond.

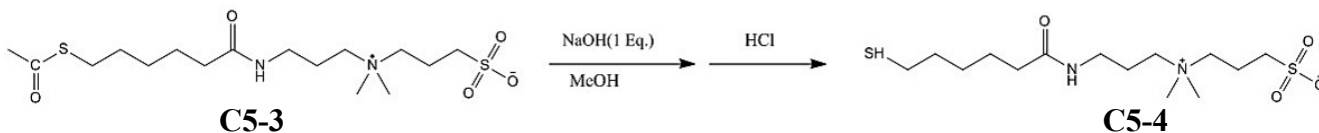


Figure S4. Deprotection step of the thiol group.

(B) Synthesis and characterisation of P12 Ligand.

The synthetic method was adopted from a previous paper in our group³. 6.9 g 1,12-dibromododecane (21.02 mmol, Acros Organics, <https://www.acros.com/>) in dry THF was added into 1.2 g of potassium thioacetate (10.51 mmol, Fisher Scientific). The mixture was then heated to reflux with stirring for 24 h under N₂ atmosphere. The reaction results in a turbid liquid. The product was then filtered and washed with 20 mL THF. The THF solution was rotary evaporated to obtain a yellowish oil, which was further purified with a silica gel column using 3:1 (v/v) then 2:1 (v/v) hexane/dichloromethane (DCM) as the eluent to give the P12-1 (2.11 g, 63.7%) as white solid.

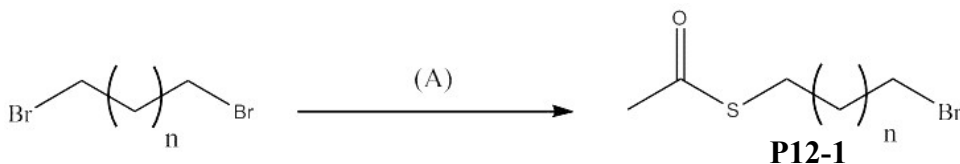


Figure S5. Replacement of bromic group with thioacetate group. (A) Potassium thioacetate/Reflux. (n = 10).

To **P12-1** (2.11 g, 6.53 mmol) in 25 mL of THF was added pyridine (2.15 g, 2.2 mL, 27.2 mmol, Alfa Aesar). After 3-day reflux, the solvent and excess reactant was removed by vacuum distillation. The residue was washed with diethyl ether (2 × 10 mL) and hexane (1 × 10 mL) and dried to obtain an orange sticky oil. The product was further purified with precipitation induced by the addition of diethyl ether to give **P12-2** (2.3 g, 80.15%) as pale brown solid.

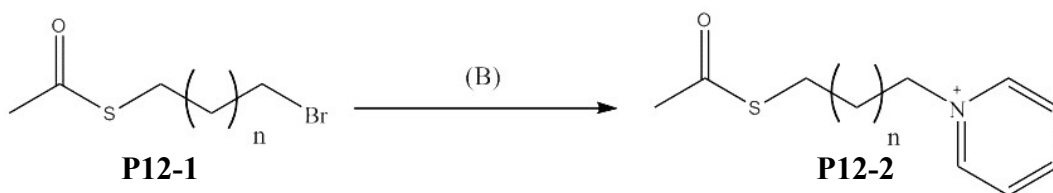


Figure S6. Mechanism of the addition of pyridine onto the alky chain. (B) Pyridine/THF and Reflux. ($n = 10$).

HBr (5.3 mL, 46.78 mmol, Honeywell, <https://lab.honeywell.com/>) was added into a mixture of MeOH and H₂O (42.0 mL, 50/50 v/v) to prepare HBr solution. **P12-2** (2.3 g, 7.13 mmol) was dissolved in the HBr solution then heated to reflux under N₂ atmosphere for 12 h. The product was rotary evaporated and purified with a typical gradient elution HPLC with methanol. **P12-3** (0.745 g, 39.6%) was obtained as light-yellow oil (turned to white waxy solid at 4 °C).

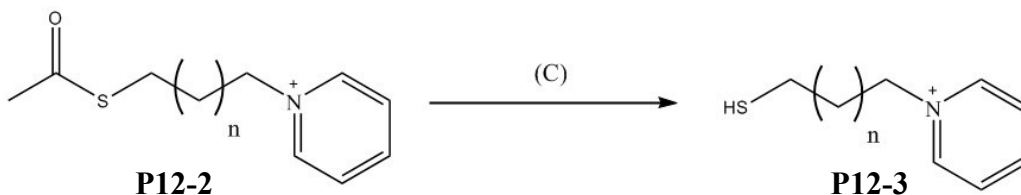
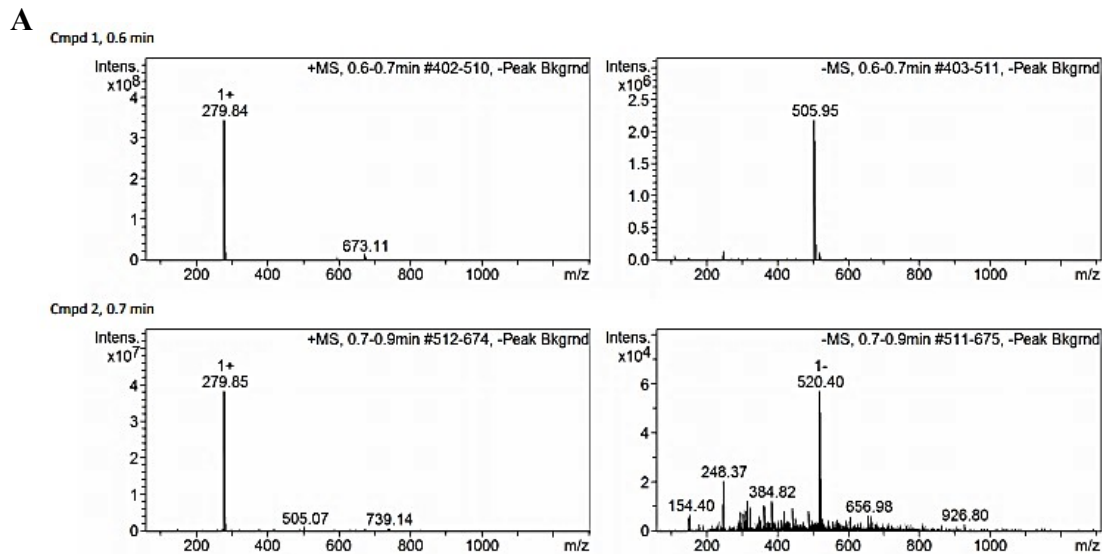
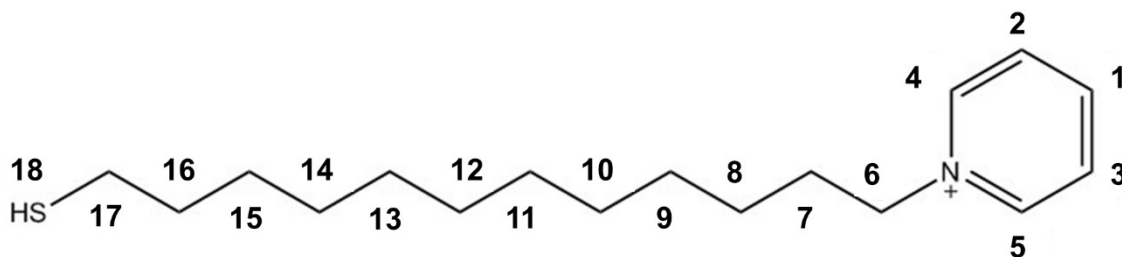


Figure S7. Deprotection of the thiol group. (C) HBr/Reflux. ($n = 10$).

The ion exchange procedure is based on a previous report⁴. After receiving the ion exchange resin (Amberlite IRA400JCL, Sigma-Aldrich, <https://www.sigmaaldrich.com/>), deionized water was applied to do rinse until the drainage is clear. Ethanol was used to soak the resin for 24 h and was renewed every 8 h. For preventing fragmentation caused by quick expansion, 25% (wt) brine was used for soaking for 12 h until it reaches the osmotic balance. The concentration was changed to 10% (wt). The expanded resin can be kept within 10% resin until the next step.

To bring enough chloride ions onto the positively charged scaffold. 4% (v/v) HCl was used to rinse and immerse the resin for 24 hours. After that, the resin was washed with deionized water until there is no detectable colour change of the pH test paper.

The ion exchange was operated in a 20 mm chromatography column. To be specific, the P12 solution was diluted to 5 mL (0.2 M) then passed through the column. The acquired liquid was put into the column again until the colour did not change. 10 mL water and 10 mL ethanol were applied to wash out all the products. The product was finally dried and lyophilized.



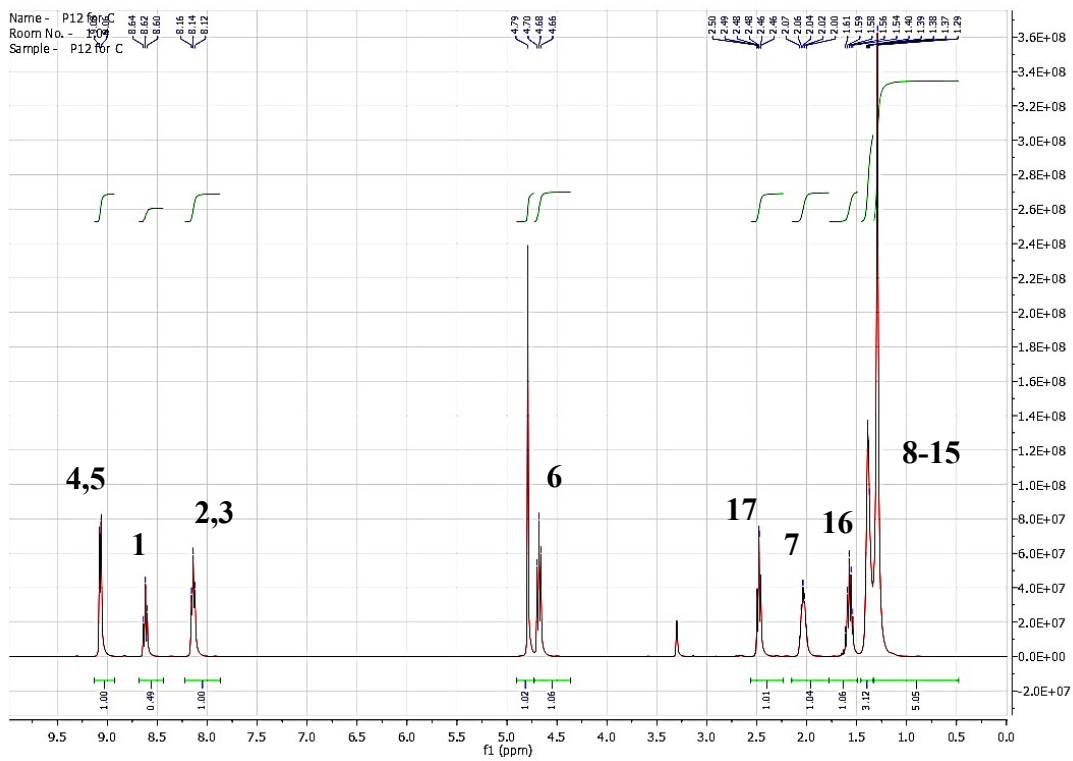
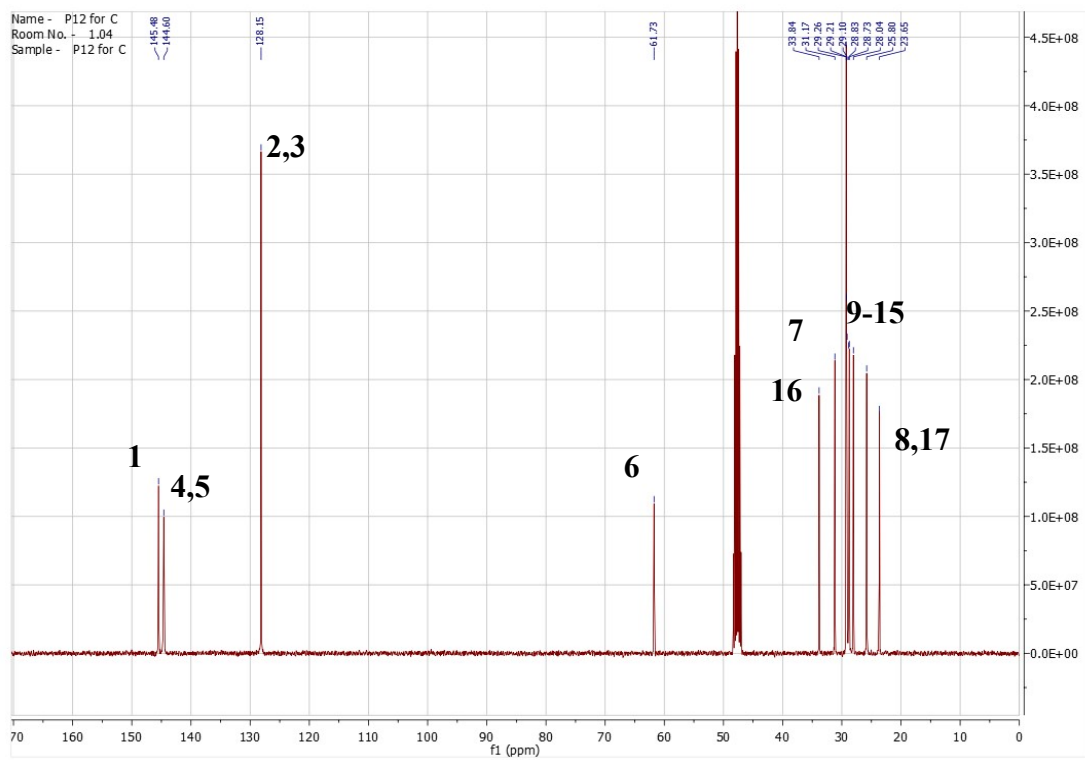
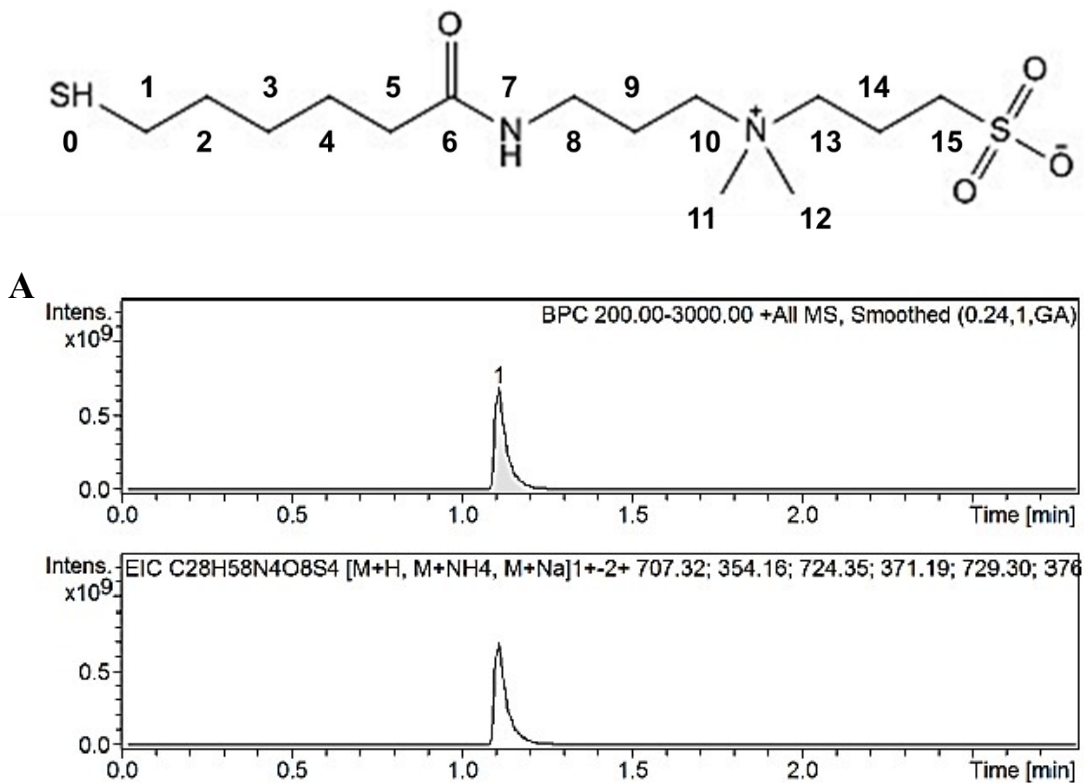
B**C**

Figure S8. (A) Mass spectrometry; (B) ^1H NMR and (C) ^{13}C NMR graphs of P12 pyridinium ligand.



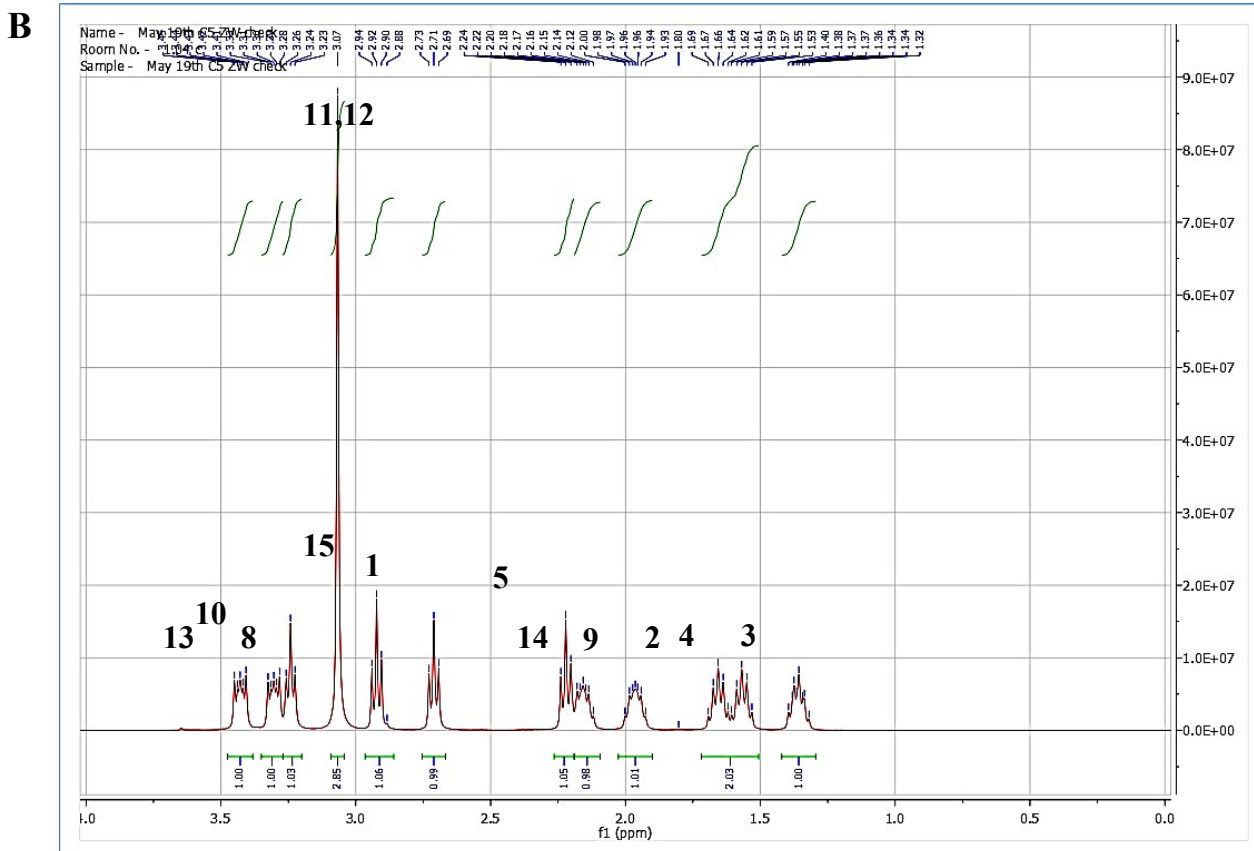


Figure S9. (A) Mass spectrometry and (B) ^1H NMR graph of C5 ZW ligand.

(C) Synthesis of $\text{Au}_{25}(\text{P12})_x(\text{C5})_{18-x}$ NCs.

The water-soluble Au_{25} NC synthetic protocol was adopted from the previous report⁵. Briefly, chloroauric acid tetrahydrate (20 mM, 250 μL , Macklin Reagent, <http://www.macklin.cn/>) was added to the desired C5 & P12 ligand solution (5 mM, 2 mL). The mixture became yellow with some turbidity, which turned to clear upon the addition of NaOH (1 M, 80 μL), followed by 2 mL ethanol. Finally, 12.5 μL NaBH_4 (100 mM in 0.2 M NaOH) was added dropwise with vigorous stirring. After 3 h, the product was purified with the 3 kDa-cutoff Amicon[®] Ultrafiltration Units (Sigma-Aldrich, <https://www.sigmaaldrich.com/>) and washed with deionized water three times.

ESI-MS data were obtained by appropriately diluting GNCs then directly injecting the sample with a syringe pump to high-resolution ESI-MS (Q-Exact[™], Thermo Fisher

Scientific). The acquired MS data were further deconvoluted with Thermo Scientific Protein Deconvolution software with an Xtract method. The output mode was MH+ with the S/N threshold set as 8. The relative abundance threshold was 5%, and the minimum number of detected charges was set to be 2. The overall charge and m/z range were set in terms of the final product condition. After getting the relationship between molecular mass and abundance, we calculated the weighted average molecular mass of the product corresponding with the P12 feed ratio.

To verify the GNC formation situation, we utilized a UV-Vis spectrometer (SHIMADZU UV-2700i, <https://www.shimadzu.com/>) to characterise the absorption curvature. We collected samples every 10 min within the first hour of the dynamic study case. After 1 h, the time interval was increased to 20 min until the end of the reaction.

The zeta potential of GNC was measured with Zetasizer Nano ZS90 (Malvern Panalytical, <https://www.malvernpanalytical.com>). The cuvette type is DTS1070.

(D) Antibacterial Tests.

Before experiments, all the bacteria species (*Staphylococcus aureus*, *Escherichia coli*, *Klebsiella pneumoniae*, *Pseudomonas aeruginosa*, *Staphylococcus epidermidis*, *Staphylococcus haemolyticus*, *Enterococcus faecium*) were selected from single colonies and pre-incubated over 24 h in LB broth (Gibco, <https://www.thermofisher.com/>). 10 μ L bacterial-containing medium was then inoculated into 1 mL fresh LB broth and incubated for another 6 h. For MRSE, its OD₆₀₀ value was around 0.3 and had a concentration of $\sim 7 \times 10^8$ CFU mL⁻¹.

The antibacterial test was carried out with the broth-dilution method⁶. On a 96-well plate, each well was filled with 100 μ L medium, and 100 μ L of undiluted GNC was introduced to the first column of wells on the left. After mixing thoroughly, 100 μ L solution from the first column was taken out and injected into the second column. This procedure was repeated to dilute the GNC in half each time. We set the very last column as a control group without the GNC. In the end, 10 μ L 1000-times diluted bacterial solution was added to each well. After 16 h and 24 h, the antibacterial result was recorded by measuring the OD₆₀₀.

Similarly, the checkerboard test was carried out with both horizontally and vertically diluting test materials and antibiotics. After 24 h of incubation, we measured the OD₆₀₀ value with a microplate reader. The FIC value that achieves more than 80% inhibition (each equivalent point) was calculated according to the following formula:

$$\Sigma FIC = FIC_A + FIC_B = \frac{C_{A \text{ combined}}}{MIC_{A \text{ single}}} + \frac{C_{B \text{ combined}}}{MIC_{B \text{ single}}}$$

In which the FICI equals the ΣFIC_{\min} . If the $FICI \leq 0.5$, then there is a synergy of both materials. If the $0.5 < FICI \leq 1^7$, then there is an additive effect of the two materials. The antibacterial tests of all Gram-positive species were carried out with the same protocol.

Time-dependent Bacterial Killing Measurement. In each well of the 96-well plate, the GNC and Imp solutions were added to make a final concentration of 16 and 2 $\mu\text{g mL}^{-1}$, respectively. The final volume was kept 100 μL per well. Logarithmic phase MRSE stock was diluted 1000 times then inoculated 10 μL into each well. At predefined time points, the solution was taken out 100 μL , appropriately diluted, and evenly applied on pre-warmed agar plates in triplicates. After 24 h incubation, the colony number on each plate was calculated to get the time-dependent bacterial killing curves.

(E) Biocompatibility Assays.

The somatic cell lines used in this study were purchased from ATCC, US. 90 μL of cell suspension (containing $\sim 2 \times 10^4$ cells) was added into each well of 96-well plates, and the plate was incubated within a cell incubator for 12 h. After cells had adhered to the plate, 10 μL of the test samples was added into each well, and cells were further incubated for 12/24 h. Then 10 μL of CCK-8 reagent (DOJINDO, <https://www.dojindo.co.jp/>) was added into each well, and cells were incubated for another 40 min. The absorbance of each well at 450 nm (OD₄₅₀) was measured on a microplate reader.

For confocal laser microscope imaging, 90 μL of 2×10^4 cell suspension was added to each 35 mm glass bottom petri dish then incubated for 12 h. 10 μL of the test material was inoculated and mixed well the culture medium then incubated for 12/24 h. The cells were taken out and stained with an adequate concentration of Calcein-AM and PI

(Keygen, <http://www.keygentec.com.cn/>) for 30 min. The confocal fluorescence images were taken with a 488 nm excitation and 515 (for Calcein-AM)/617 (for PI) nm emission. The cell counting was operated with a Countess™ II Automated Cell Counter (Thermo Fisher, <https://www.thermofisher.com/>) with cell suspension.

Haemolytic Assay. The haemolytic study was conducted following a reported method⁶. Fresh pig whole blood (YUANYE, <http://www.shyuanye.com/>) was slightly stirred with a glass rod to remove fibrinogen, separated into 2 mL tubes. PBS buffer was added to each tube. After centrifugation at 2500 rpm for 5 min, the supernatant with plasma was discarded, and this procedure was repeated three times until the supernatant was clear. The resulting concentrated red blood cell suspension was diluted to 4% red blood cell suspension. GNCs were diluted to 500 μ L to make the desired concentrations and added the same amount of red blood cell suspension. The mixture was incubated in a 37 °C water bath for 3 h. Triton-X and PBS buffer were used as positive and negative controls. After 3 h, the tubes were centrifugated at 1500 rpm for 15 min. The supernatants were transferred to the wells of a microtiter plate, and the absorbance (A) at 540 nm (A_{540}) was measured on a microplate reader. The haemolytic rate (HL) was calculated via the equation below:

$$HL = \frac{A_{sample} - A_{negative}}{A_{positive} - A_{negative}} \times 100\%$$

Typically, a 5% haemolytic rate, referred to as HD₅, is the criteria used to compare the toxicity of different materials toward red blood cells.

(F) Antibacterial Mechanism Research.

SEM Imaging. We cultivated bacteria to logarithmic period and diluted the solution to 100-fold. Then we put coverslips into a 12-well plate and added 1.5 mL bacteria solution to let bacteria stick to the slides for 5 h. After rinsing with PBS buffer, we added GNC solution and antibiotic solution into each well and cultivated 24 h. After the incubation, bacteria in each well were rinsed again and fixed with 2.5% glutaraldehyde solution. After 12 h, plankton bacteria and bacteria metabolites were removed with PBS buffer

rinse for 3 times, 30%, 50%, 70%, 80%, 90%, 95% ethanol solutions were used for the gradient dehydration for 15 min each. Finally, we added pure ethanol into each well and let the sample dry naturally before SEM imaging (Merlin SEM, ZEISS, <https://www.zeiss.com/>).

Analysis of ROS Generation Rate and Type. The Reactive Oxygen Detection Kit (Beyotime, <https://www.beyotime.com/>) was used to detect ROS levels. The DCFH-DA (2,7-Dichlorodi-hydrofluorescein diacetate) solution was diluted with PBS 1000 times to 10 μ M working solution. The logarithmic phase MRSE was washed with a PBS solution twice, and the proper amount of working solution was added to resuspend the bacteria. The solution was mixed every 3-5 min to make it thoroughly blended. After 30 min, the solution was washed with PBS and mixed with the GNC and antibiotics. The fluorescent readout was carried out after 1 h incubation with 488 nm excitation and 525 nm emission with a plate reader (Synergy H1, BioTek, <https://www.biotek.com/>). The ROS species were detected with the GENMED Bacterial ROS (hydroxyl radical) quantitative detection kit (colourimetric) and the GENMED ROS (superoxide anion) quantitative detection kit [colourimetric, nitro-blue tetrazolium (NBT) method] (GENMED, <http://genmedsci.com/>).

Membrane Penetration Assay. The membrane integrity was analysed by BBcellProbe™ Colourimetric Cell Membrane Integrity Test Kit (BestBio, <http://www.bestbio.com.cn/>). The working solution of membrane integrity staining T12 dye was prepared by diluting the stock solution 50-500 times. Pre-treated MRSE cells within centrifugation tubes were washed by PBS twice, followed by adding the working solution and resuspension of MRSE cells. After 10 min of incubation, the mixture was re-washed with PBS 3 times. The final absorption value was measure with a microplate reader at 620 nm.

Analysis of GNC Binding with WTA. The WTA used in the experiments was extracted from *S. aureus* following a former report⁸. The isothermal titration was performed by adding 1.1 mg mL⁻¹ WTA dropwise into the 1.4 mL 200 μ g mL⁻¹ GNC within the chamber (MicroCal VP-ITC, GE, <https://www.ge.com/>). The total injections were 27 times, with 10 μ L each. The titration duration was 20 s and the time spacing was 150 s. The interference was eliminated with the subtraction of pure WTA titration.

To further illustrate the GNC binding with WTA, a competitive fluorescence experiment was conducted by following a former protocol with minor modifications⁹. The working solutions of BODIPYTM-TR-cadaverine (10 mM, J&K Scientific, <https://www.jk-scientific.com/>) and WTA (14 $\mu\text{g mL}^{-1}$) were previously diluted with Tris-buffer (50 mM, pH 7.4). The final concentrations of BODIPYTM-TR-cadaverine and WTA were 5 μM and 3.5 $\mu\text{g mL}^{-1}$, respectively. After 15 min of reaction, the GNC was added, followed by 30 min incubation at 25 °C. The whole procedure was protected from light. The fluorescence was measured using the excitation and emission wavelengths of 580 nm and 620 nm, respectively.

Molecular Binding Simulation. The simulation of WTA was based on reference¹⁰. Molecular dynamics (MD) simulations were performed in Amber 99sb-ILDN force field by GROMACS. We optimized the structure of the GNC and got the equilibrated conformation. The optimized GNC structure was then put on the WTA surface at 1.5 nm apart, allowing the GNC to move randomly. The time duration of 60 ns and 30 ns with a coupling constant of 2 fs at a constant temperature of 298.15 K was used for the (isothermal–isobaric) NPT ensemble GNC and the GNC-WTA systems, respectively. We calculated bond lengths and long-distance electrostatic interactions with the SHAKE algorithm and particle mesh Ewald method, and only the last 5 ns of each simulation was used for analysis. The generated trajectories were evaluated using GROMACS inbuilt tools, and the results were visualized using VMD.

Detection of Bacterial Membrane Potential Change. Bacterial membrane potential assay was performed with MycoLightTM Ratiometric Bacterial Membrane Potential Kit (AAT Bioquest, <https://www.aatbio.com/>) and followed the instructions. MRSE in the logarithmic phase was diluted to $\sim 1 \times 10^6$ cells per mL and divided into 500 μL aliquots in centrifugation tubes. GNC and Imp solutions were added into tubes and incubated for 2 h; 10 μL of carbonyl cyanide *m*-chlorophenyl hydrazone (CCCP) (500 μM) was used as the positive control. 5 μL of MycoStain ItTM Green (10X) were added into each tube successively and mixed. The samples were incubated at room temperature for 30 min before their confocal fluorescence images were collected using a 488 nm excitation and 530, 610 nm emission, respectively. The red/green ratio was measured with ImageJ.

Stability Study of GNC in Biological Fluid. The experiment was performed to rule out the possibility of aggregation or ligand shedding-induced fluorescent quenching. Briefly, GNC (final concentration as $128 \mu\text{g mL}^{-1}$) was added to PBS and human serum albumin (HSA) solutions (2.5%, 5%, 10%, final concentration) and mixed. The fluorescence images were measured daily within half a month with a NIR animal imager (Series III 900/1700, NIROPTICS, <http://www.nir-optics.com/>).

(G) Animal Tests.

All animal studies were conducted according to the approved protocols by the Institutional Animal Care and Use Committee, Shenzhen Advanced Animal Study Service Centre (IACUC, IRB Number: AASC200615M).

The GNC *In Vivo* Biosafety Assay. The biosafety test was performed with evenly-grouped 36 BALBc mice (female, 6 weeks old, SPF grade). Before injection, the test subjects were evenly grouped ($n = 4$), shaved, and fasted over 12 h. 5 mg kg^{-1} GNC and 1.28 mg kg^{-1} Imp (final concentration) mixed solution was applied $200 \mu\text{L}$ while $200 \mu\text{L}$ PBS was applied to the control group through tail vein injection. At different time points, organs of one group of mice were dissected to characterise the GNC accumulation under the same imaging condition. The fluorescence image was monitored with the NIR animal imager using an 808 nm laser excitation and a 1020 nm emission filter. The power of the laser source is 5 W.

To acquire the Au content in the main organs, the main organs were taken out, thawed, washed with PBS buffer, and ground to slurry with a tissue grinder separately. The masses of the organs were recorded. Aqua regia (3:1 v/v of concentrated HCl and HNO_3) was freshly prepared and added to each vial containing tissue homogenate. After a 12 h incubation, each vial mixture was heated to $>100 \text{ }^\circ\text{C}$ until the aqua regia was evaporated and tissue fully incinerated. The remnant was re-dissolved in water, diluted, and analysed with an inductively coupled plasma-mass spectrometry (ICP-MS, Agilent 7700, <https://www.agilent.com/>) to measure the Au content. After 3 days, we collected blood samples of the experiment and control groups, then did a routine blood test and blood biochemical analysis to confirm the safety of the combination.

Skin Infection Model. The animal test was based on a previous report with modifications^{11,12}. Sprague Dawley rats (female, 8 weeks old, ~250 g) were divided evenly ($n = 3$). Three whole-sized wounds ($d = 1.5$ cm) were created at the back of each rat, and 150 μL MRSE bacteria solution ($\sim 1 \times 10^9$ CFU mL^{-1}) was spread evenly on the wound. After 1 h infection, 100 μL PBS, 24 $\mu\text{g mL}^{-1}$ Imp solution, 64 $\mu\text{g mL}^{-1}$ GNC solution, and the combination of 24 $\mu\text{g mL}^{-1}$ Imp (~ 0.12 mg kg^{-1} , final concentration) and 64 $\mu\text{g mL}^{-1}$ GNC solution (~ 0.32 mg kg^{-1} , final concentration) were spread on the wounds of each group, respectively. The wound size and wound bacteria number were recorded every three days. On day 6 and day 12, wounds were randomly dissected from rats and fixed with 4% paraformaldehyde solution for the subsequent H&E staining.

Pathology. Fixed tissue specimens were cut, trimmed into blocks. The tissue was dehydrated in a gradient alcohol solution, embedded in paraffin, and sliced with a Leica 2235 microtome (<https://us.leica-camera.com/>) into 4 μm thick sections. For H&E staining, paraffin sections were dewaxed three times, rehydrated with a gradient alcohol solution, rinsed, and stained with hematoxylin dye and eosin dye solution (Solarbio, <http://www.solarbio.com/>) in order. After that, sections were gradient dehydrated again, transparentized with xylene, and sealed with neutral resin glue. The tissue slices were observed with CaseViewer.

II. MATERIAL CHARACTERISATION

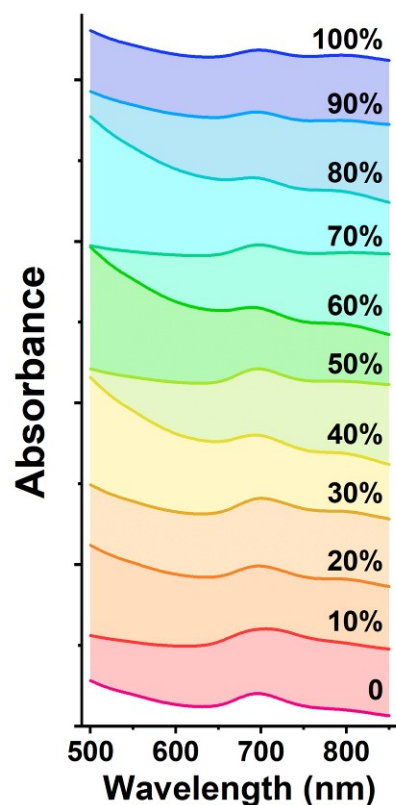


Figure S10. A collection of UV-vis absorption spectra demonstrating the absorption peaks of $\text{Au}_{25}(\text{P12})_x(\text{C5})_{18-x}$ GNCs prepared with different P12 ligand feed ratios. The unanimous peak position has confirmed their structures to be identical.

Table S1. Theoretical molecular weight of $\text{Au}_{25}(\text{P12})_x(\text{C5})_{18-x}$ prepared with different P12/C5 collocation ratios.

The GNC structure $\text{Au}_{25}(\text{P12})_x(\text{C5})_{18-x}$	Corresponding GNC molecular weight (Da)
$\text{Au}_{25}(\text{P12})_0(\text{C5})_{18}$	11282
$\text{Au}_{25}(\text{P12})_1(\text{C5})_{17}$	11208
$\text{Au}_{25}(\text{P12})_2(\text{C5})_{16}$	11134
$\text{Au}_{25}(\text{P12})_3(\text{C5})_{15}$	11061

$\text{Au}_{25}(\text{P12})_4(\text{C5})_{14}$	10987
$\text{Au}_{25}(\text{P12})_5(\text{C5})_{13}$	10914
$\text{Au}_{25}(\text{P12})_6(\text{C5})_{12}$	10840
$\text{Au}_{25}(\text{P12})_7(\text{C5})_{11}$	10766
$\text{Au}_{25}(\text{P12})_8(\text{C5})_{10}$	10693
$\text{Au}_{25}(\text{P12})_9(\text{C5})_9$	10619
$\text{Au}_{25}(\text{P12})_{10}(\text{C5})_8$	10545
$\text{Au}_{25}(\text{P12})_{11}(\text{C5})_7$	10472
$\text{Au}_{25}(\text{P12})_{12}(\text{C5})_6$	10398
$\text{Au}_{25}(\text{P12})_{13}(\text{C5})_5$	10324
$\text{Au}_{25}(\text{P12})_{14}(\text{C5})_4$	10251
$\text{Au}_{25}(\text{P12})_{15}(\text{C5})_3$	10177
$\text{Au}_{25}(\text{P12})_{16}(\text{C5})_2$	10103
$\text{Au}_{25}(\text{P12})_{17}(\text{C5})_1$	10030
$\text{Au}_{25}(\text{P12})_{18}(\text{C5})_0$	9956

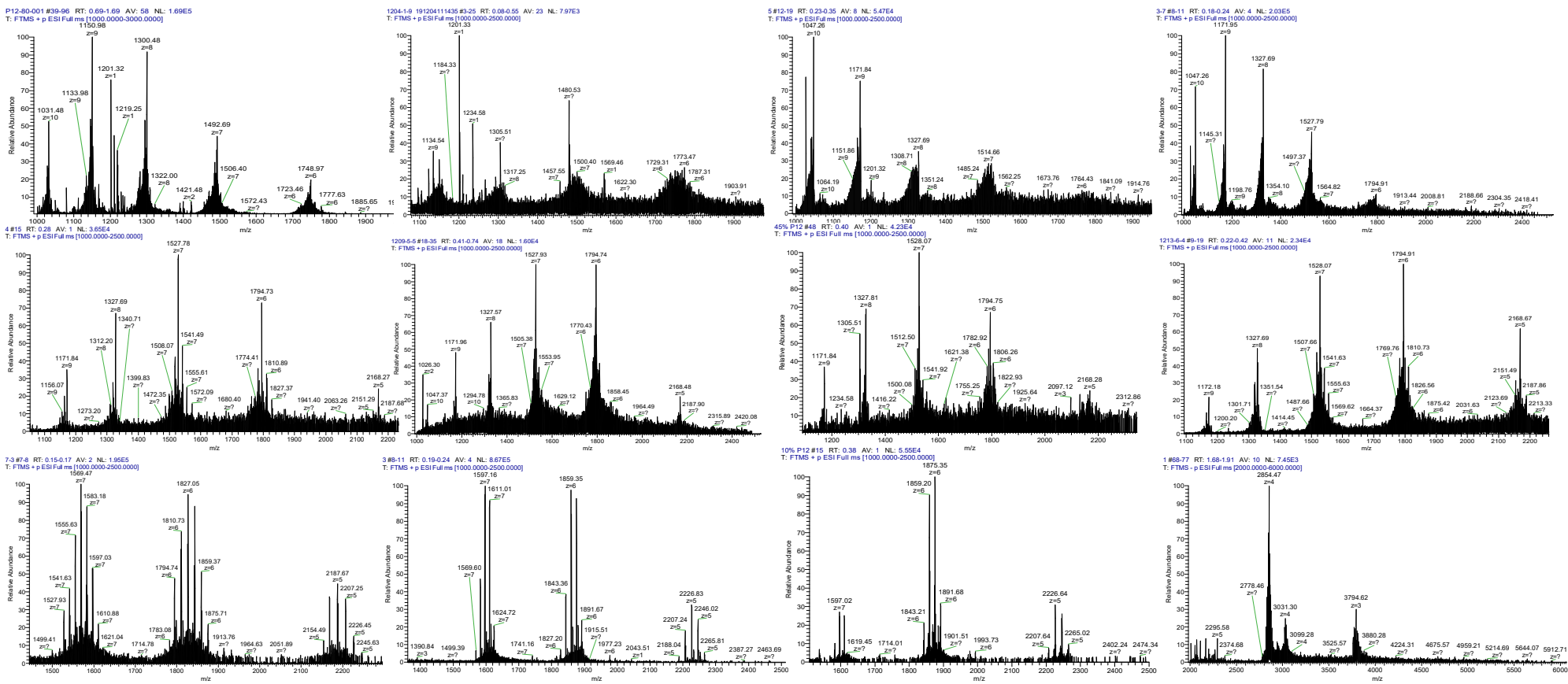


Figure S11. ESI-MS graphs of GNCs with different P12 ligand feed ratio. (From left to right, top to bottom: 100%, 90%, 80%, 70%, 60%, 50%, 40%, 30%, 20%, 10%, 0%).

III. ANTIBACTERIAL AND BIOCOMPATIBILITY TESTS

Table S2. 24-h antibacterial result of different formulated GNCs toward five common pathogens (the colour scale represents the antibacterial effect: the red stands for high, the yellow stands for medium, the green represents low, and the grey represents negligible).

P12 ratio in feeding (%)	MIC ($\mu\text{g mL}^{-1}$)				
	<i>E. coli</i>	<i>K. pneumoniae</i>	<i>P. aeruginosa</i>	<i>S. aureus</i>	MRSA
0	>128	>128	>128	>128	>128
10	>128	>128	128	128	128
20	>128	128	64	128	64
30	>128	>128	64	64	64
40	>128	>128	128	32	64
45	64	128	64	16	32
50	32	64	16	32	16
60	128	128	32	32	32
70	64	64	32	32	32
80	64	64	32	32	32
90	32	64	16	32	32
100	32	64	32	16	16

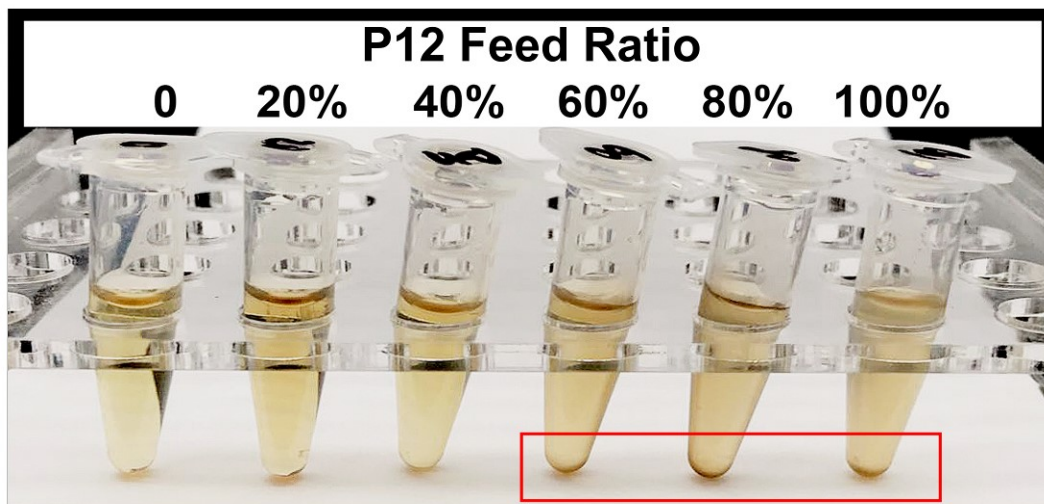


Figure S12. Photo of GNCs (all $128 \mu\text{g mL}^{-1}$) with increasing P12 feed ratio in LB broth. Aggregation was observed for GNCs prepared with $\geq 60\%$ P12 ligand but not for those prepared with $\leq 40\%$ P12 ligand (labelled with red box).

P12 Feed ratio

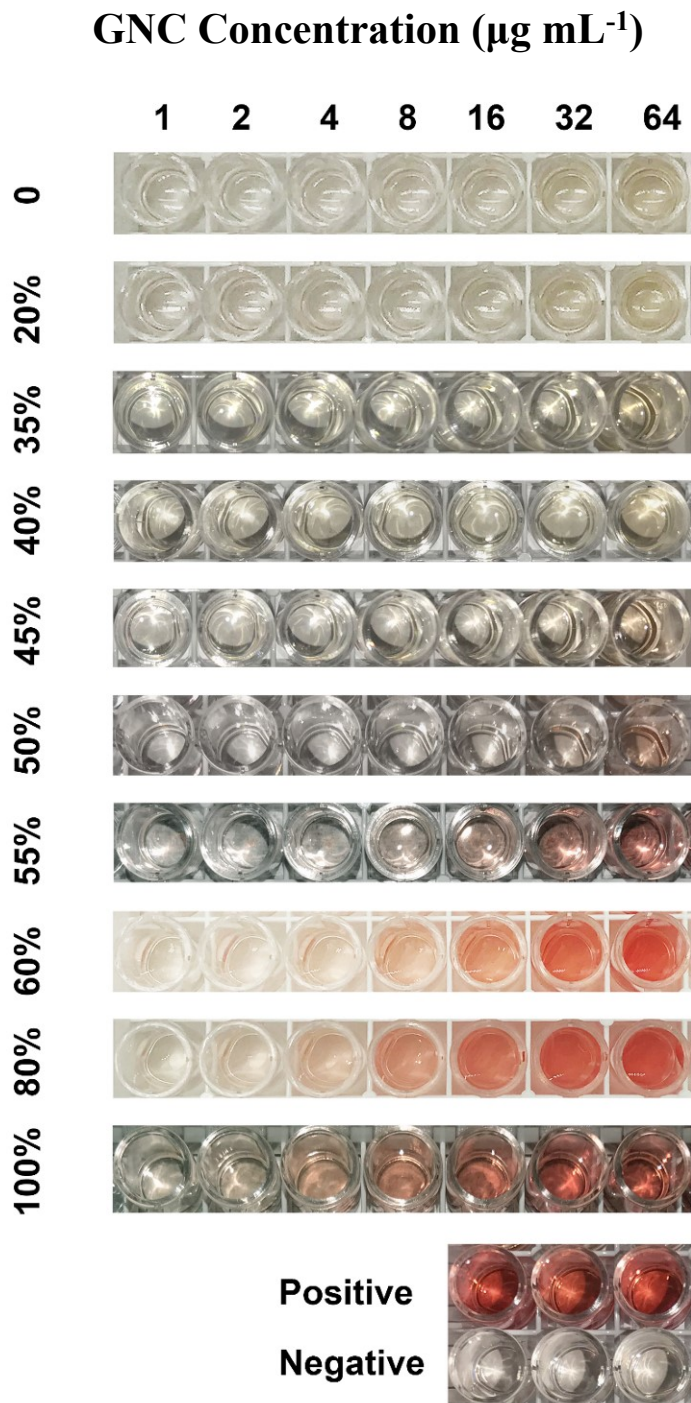


Figure S13. Haemolytic figures of GNCs with different P12 feed ratios.

Table S3. Comparison of MIC values of seven antibiotics used to treat Gram-positive bacterial infections from four main categories: β -lactams [Ampicillin (AMP), Oxacillin (Oxa), Penicillin (Pen), Imipenem (Imp)], glycopeptide [Vancomycin (Van)], macrolides [Erythromycin (Ery) and Azithromycin (Azi)], and tetracycline [Tetracycline (Tet)] against a clinically isolated strain of MRSE.

Antibiotics	Amp	Oxa	Pen	Imp	Van	Ery	Tet	Azi
MIC values ($\mu\text{g mL}^{-1}$)	32	>128	64	64	2	32	≤ 1	>128

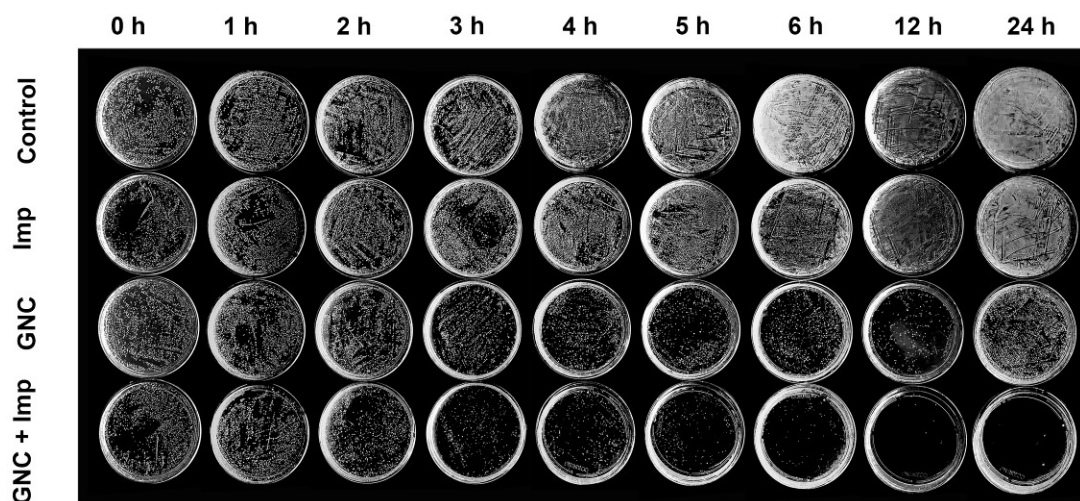


Figure S14. The undiluted time-dependent bactericidal results of treatments with the PBS buffer (control), Imp only ($2 \mu\text{g mL}^{-1}$), GNC only ($16 \mu\text{g mL}^{-1}$), and a combination of GNC ($16 \mu\text{g mL}^{-1}$) and Imp ($2 \mu\text{g mL}^{-1}$) to visually display changes in colonies.

IV. ANTIBACTERIAL MACHENISM ILLUSTRATION

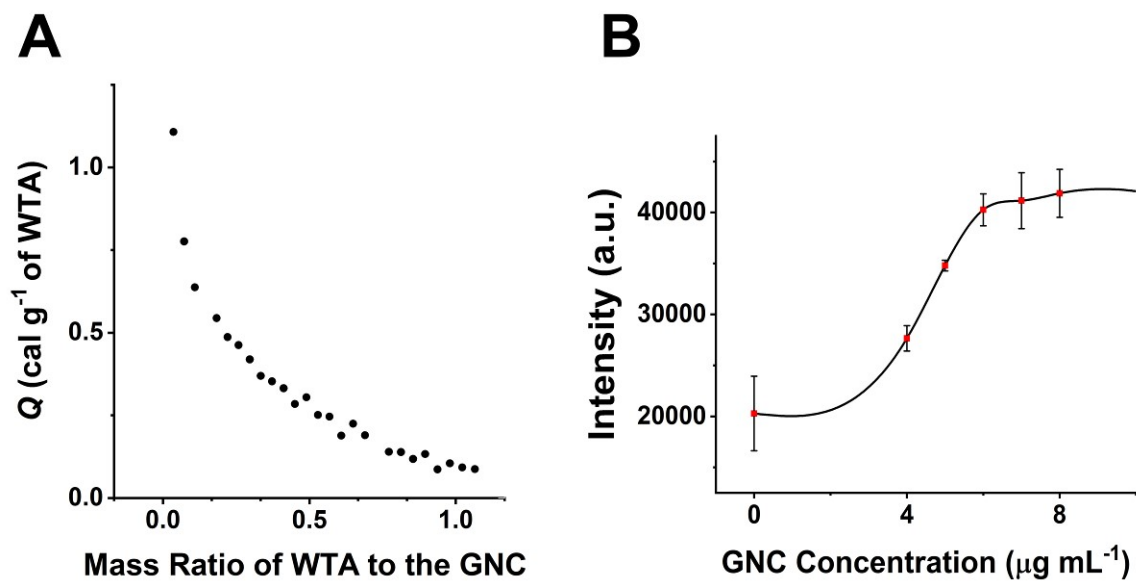


Figure S15. (A) Isothermal titration calorimetry (ITC) result for specific binding between GNCs and WTA. (B) Plot of fluorescent intensity vs. GNC. With an increase in the GNC concentration, the fluorescence emitted by the free TR-cadaverine was enhanced until saturation ($n=4$).

V. BIOSAFETY AND *IN VIVO* DISTRIBUTION EXPERIMENTS

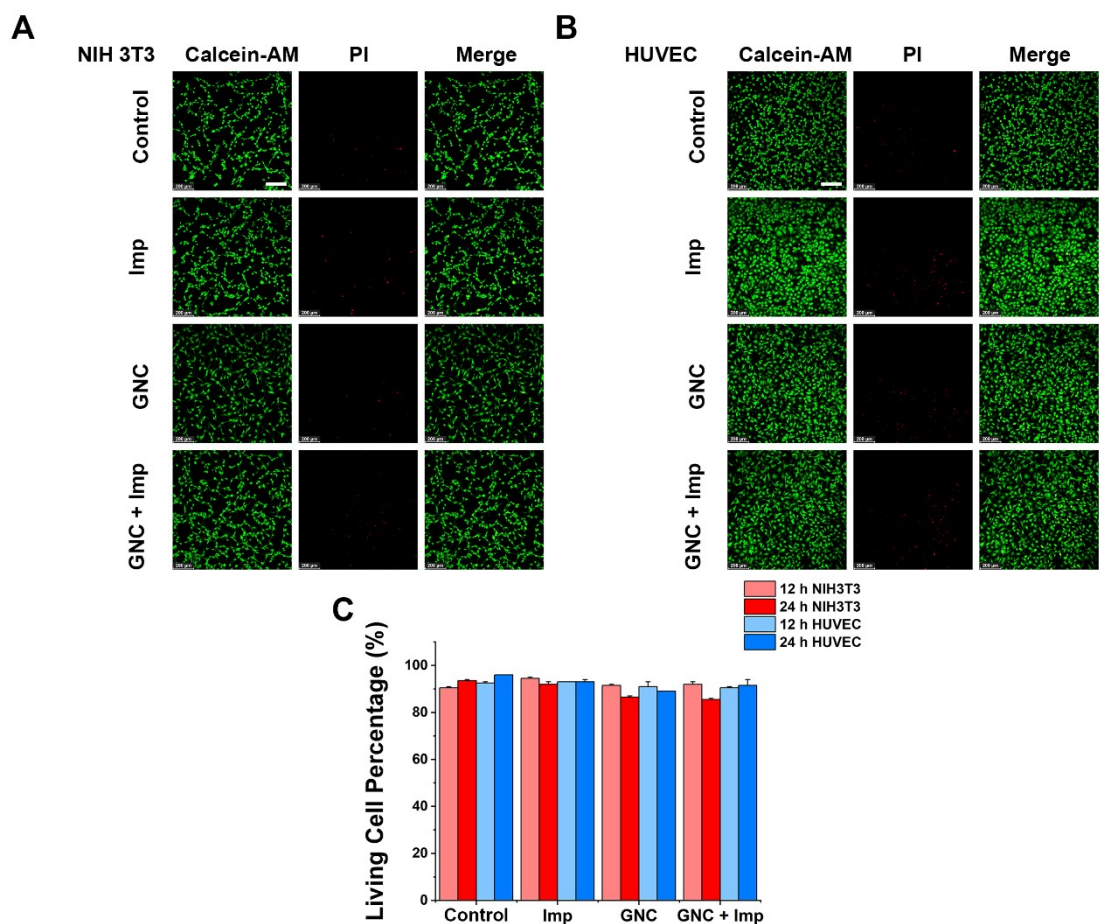


Figure S16. Biocompatibility evaluation of the GNC + Imp combination treatment. (A) Confocal fluorescence images of NIH 3T3 cells after a 24-h incubation in PBS (control), $70 \mu\text{g mL}^{-1}$ GNC, $30 \mu\text{g mL}^{-1}$ Imp and $70 \mu\text{g mL}^{-1}$ GNC + $30 \mu\text{g mL}^{-1}$ Imp, (scale bar: $200 \mu\text{m}$). (B) Confocal fluorescence images of HUVECs after 24 h incubation in PBS, $70 \mu\text{g mL}^{-1}$ GNC, $30 \mu\text{g mL}^{-1}$ Imp, and $70 \mu\text{g mL}^{-1}$ GNC + $30 \mu\text{g mL}^{-1}$ Imp, Scale bar: $200 \mu\text{m}$). (C) Cell-counting results reflecting the viability of the two cell lines in $70 \mu\text{g mL}^{-1}$ GNC and $30 \mu\text{g mL}^{-1}$ Imp for 12 and 24 h ($n=3$).

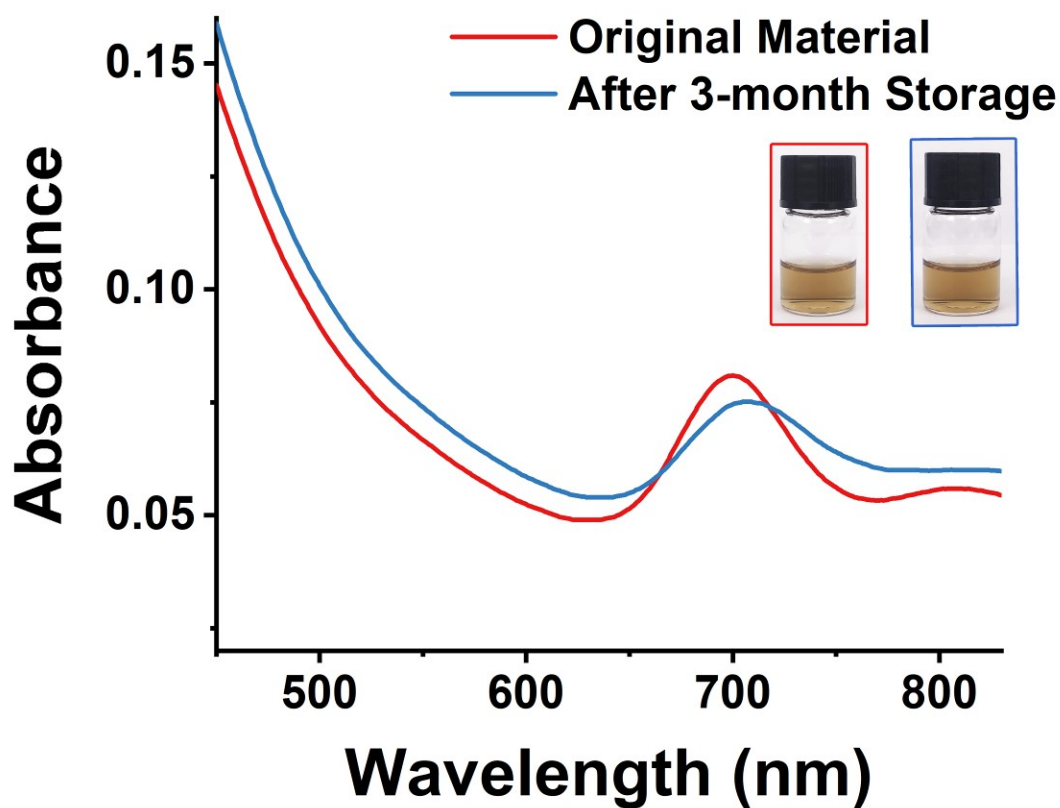


Figure S17. Comparison of the UV-vis spectrum of the GNC after 3-month storage at 4 °C. The corresponding physical photos are also displayed. After 3 months, except for a slight red-shift of the characteristic peak position, the overall shape remained unchanged. In addition, the colour and clarity were consistent with the original material, with no precipitation or character changes.

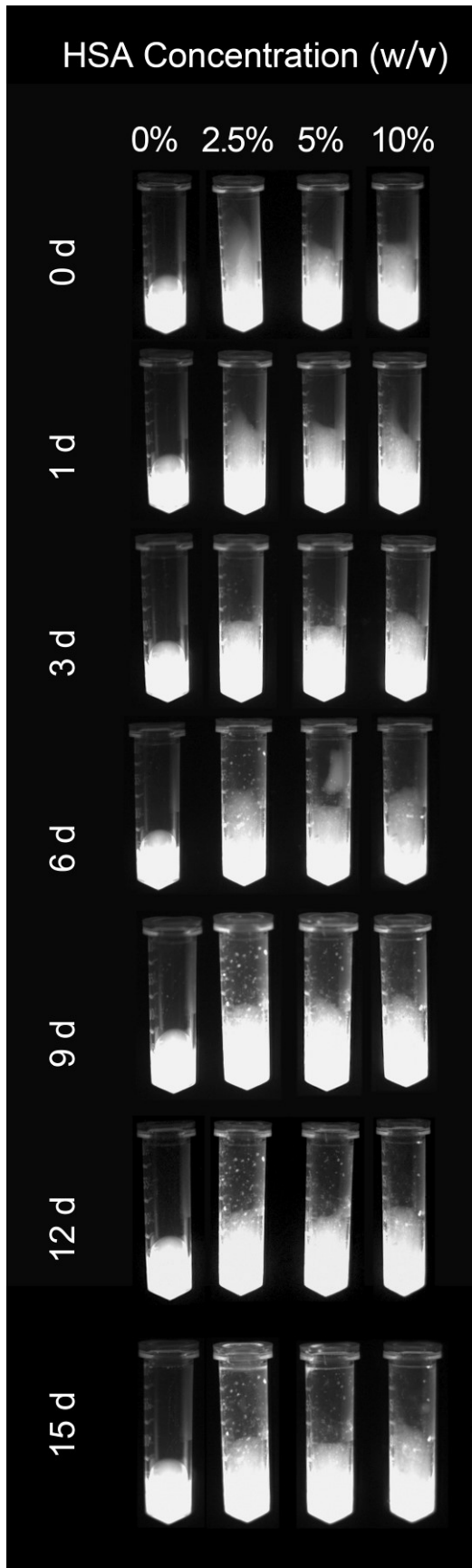


Figure S18. NIR fluorescence images of the GNC ($128 \mu\text{g mL}^{-1}$) in PBS solutions containing 0, 2.5%, 5%, and 10% HSA over 15 days. No change in fluorescence intensity was observed.

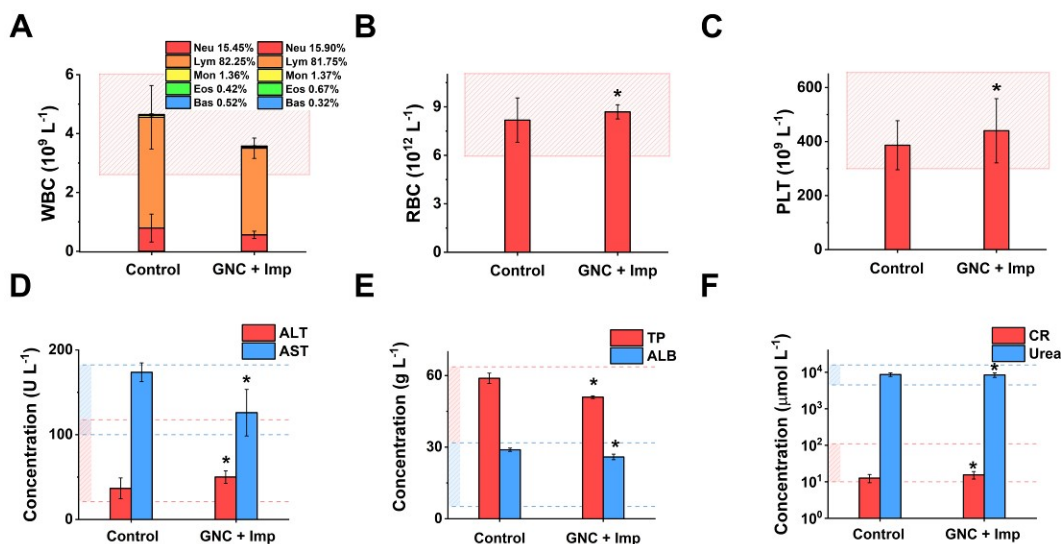


Figure S19. Blood routine tests of the (A) white blood cell (WBC) quantity and composition analysis (* $P > 0.05$, same below). (B) red blood cell and (C) platelet quantity analysis of different groups. Comparison of liver and kidney function indicators (D) alanine aminotransferase (ALT) aspartate aminotransferase (AST); (E) total protein (TP), albumin (ALB); (F) creatinine (CR) and urea nitrogen (Urea) concentration between the GNC+Imp and the control group ($n=3$). The reference ranges are marked, and the sample results of all experimental groups are within the normal range.

VI. REFERENCES

- 1 D. Mishra, S. Wang, Z. Jin, E. Lochner and H. Mattoussi, *ChemRxiv.*, 2018.
- 2 G. W. Anderson and R. Paul, *J. Am. Chem. Soc.*, 1958, **80**, 4423.
- 3 D. Zhou, X. Wang, L. Birch, T. Rayment and C. Abell, *Langmuir.*, 2003, **19**, 10557–10562.

- 4 Y. Ishida, K. Narita, T. Yonezawa and R. L. Whetten, *J. Phys. Chem. Lett.*, 2016, **7**, 3718–3722.
- 5 T. Chen, V. Fung, Q. Yao, Z. Luo, D. E. Jiang and J. Xie, *J. Am. Chem. Soc.*, 2018, **140**, 11370–11377.
- 6 Y. Xie, Y. Liu, J. Yang, Y. Liu, F. Hu, K. Zhu and X. Jiang, *Angew. Chemie - Int. Ed.*, 2018, **57**, 3958–3962.
- 7 L. A. Barbee, O. O. Soge, K. K. Holmes and M. R. Golden, *J. Antimicrob. Chemother.*, 2014, **69**, 1572–1578.
- 8 T. C. Meredith, J. G. Swoboda and S. Walker, *J. Bacteriol.*, 2008, **190**, 3046–3056.
- 9 J. Swain, M. El Khoury, A. Flament, C. Dezanet, F. Briée, P. Van Der Smissen, J. L. Décout and M. P. Mingeot-Leclercq, *Biochim. Biophys. Acta - Biomembr.*, 2019, **1861**, 182998.
- 10 E. R. Caudill, R. T. Hernandez, K. P. Johnson, J. T. O'Rourke, L. Zhu, C. L. Haynes, Z. V. Feng and J. A. Pedersen, *Chem. Sci.*, 2020, **11**, 4106–4118.
- 11 M. Chen, Z. Long, R. Dong, L. Wang, J. Zhang, S. Li, X. Zhao, X. Hou, H. Shao and X. Jiang, *Small.*, 2020, **16**, 1–11.